Early View publication on
www.interscience.wiley.com
(issue and page numbers not yet assigned;
citable using Digital Object Identifier – **DOI**)

J. Biophoton. 1–10 (2009) / **DOI** 10.1002/jbio.200810057

Journal of
BIOPHOTONICS

FULL ARTICLE

Spectroscopy on the wing: Naturally inspired SERS substrates for biochemical analysis

Natalie L. Garrett, Peter Vukusic, Feodor Ogrin, Evgeny Sirotkin, C. Peter Winlove, and Julian Moger*

School of Physics, University of Exeter, Devon, UK, EX4 4QL, UK

Received 18 September 2008, revised 13 November 2008, accepted 1 December 2008
Published online 28 December 2008

Key words: butterfly, surface-enhanced Raman spectroscopy, biomimetic, biotin, assay, avidin, structure and bonding

PACS: 33.20.Fb, 78.30.–j, 81.07.–b, 87.15.By

We show that naturally occurring chitinous nanostructures found on the wings of the Graphium butterfly can be used as substrates for surface-enhanced Raman scattering when coated with a thin film of gold or silver. The substrates were found to exhibit excellent biocompatibility and sensitivity, making them ideal for protein assaying. An assay using avidin/biotin binding showed that the substrates could be used to quantify protein binding directly from changes in the surface-enhanced Raman scattering (SERS) spectra and were sensitive over a concentration range comparable with a typical enzyme-linked immunosorbent assays (ELISA) assay. A biomimetic version of the wing nanostructures produced using a highly reproducible, large-scale fabrication process, yielded comparable enhancement factors and biocompatibility. The excellent biocompatibility of the wings and biomimetic substrates is unparalleled by other lithographically produced substrates, and this could pave the way for widespread application of ultrasensitive SERS-based bioassays.

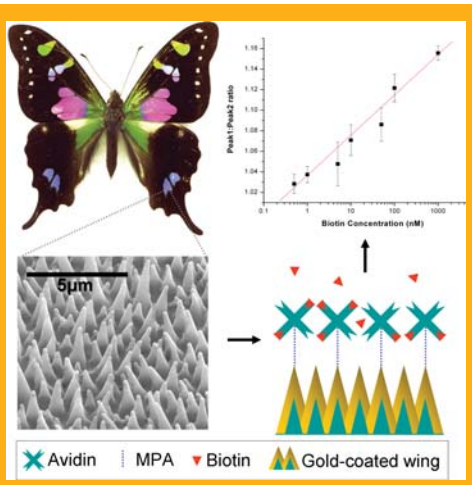

Butterfly wing to biotin assay: a schematic diagram illustrating avidin conjugation to silvered butterfly wings, together with the subsequent SERS biotin assay data.

1. Introduction

Assaying using protein binding is a powerful analytical tool that has found a wide range of applications across many market sectors. These include clinical diagnostics, pharmaceuticals, forensic and environmental evaluation and biochemical studies [1–3]. Advances in biochemistry biosensing processes have made assaying common place; for example, home pregnancy, blood glucose, and allergy testing kits are

* Corresponding author: e-mail: n.l.garrett@exeter.ac.uk

all based upon antibody assay technology. In spite of this progress, there are still significant requirements for improvements to current assay methods used in industry. The demand for improved sensitivity, throughput, specificity, and cost efficiency in industry constantly drive advances in assay technology.

Many different approaches have been successfully exploited for the detection of protein-binding events, such as: scintillation counting, fluorescence, absorption, electrochemistry, chemiluminescence, Rayleigh scattering and Raman scattering [1, 4]. Among these, fluorescence has been the most widely used readout method for industrial application, frequently in enzyme-linked immunosorbent assays (ELISA) [4], since high sensitivity is critical for the immunoassay detection. However, fluorescence-based readouts rely upon an extraneous fluorescent label that can alter binding interaction and can be unreliable when assaying in the presence of autofluorescent or scattering compounds [5].

Surface-enhanced Raman scattering (or SERS) was first discovered by Fleischmann et al. in 1974 [6] and has emerged as a powerful analytical tool. SERS is an extension of standard Raman scattering, a vibrational spectroscopic technique that provides detailed structural information about an analyte at the molecular level. Recently, several reports have demonstrated the potential of surface-enhanced Raman scattering (SERS) as a label-free readout for monitoring protein-binding events [1, 2, 7].

SERS combines Raman scattering with the exciting properties of metallic nanostructures to achieve a very significant amplification of the Raman signal: as high as 14 orders of magnitude having been reported [8]. The Raman signal of molecules adsorbed onto a 'SERS-active' metallic structure is enhanced by the localized concentrated electromagnetic fields, often referred to as 'hot-spots', due to the excitation of surface plasmons on the metal surface [9]. Initial SERS work utilized chemical roughening of metal surfaces of electrodes [6, 10, 11] and metallic colloidal conjugates [11–14], but these were found to exhibit poor reproducibility. Recent progress in nanoscience has led to highly reproducible techniques for fabricating complex nanostructures for SERS. These techniques include use of electron-beam lithography, chemical etching, colloid immobilization, annealing of metal-ion-implanted silicon, and nanosphere lithography [15–19]. They are, however, generally prohibitively expensive, complex and ultimately unsuitable to mass production. Since the substrates nanostructures are too delicate to withstand cleaning, they are only suitable for single use. For these reasons, cheaper, faster and more reproducible manufacturing processes are required.

The potential for low detection limits and higher sensitivities available with SERS have been exploited in recent biological assay research [20–22], but this has been limited by the substrates available for aqueous experiments. Many available SERS substrates require the analyte to be deposited and dried prior to scanning. This is unsuitable for most biological analytes, such as proteins, since the process of desiccation alters their configuration and hence their Raman spectrum [23]. Drop-coated deposition has been claimed to produce normal Raman spectra of proteins analogous to those obtained from aqueous proteins [24] by providing a "natural" environment. However, because protein structure is strongly dependent upon the hydration of the molecule, it is essential that aqueous conditions are maintained in order to perform rigorous investigation of biological proteins. Protein-binding systems involve complex interactions that require optimal protein structure for binding to occur. Variation in pH, hydration and temperature can have an adverse effect on protein structure, thus preventing binding events that can lead to a dramatic reduction in the detection threshold [3].

SERS assays using proteins have historically required highly complex systems with multiple interactions to produce a detectable event [1, 2], usually with colloidal noble-metal particles or a SERS chemical label providing the means of detecting binding events. These assays can provide high sensitivity to low levels of analyte in solution, but the interaction of metal colloids and chemical SERS marker molecules has the potential to adversely affect the biological molecules of interest. Intricate multiple-stage assays are undesirable for complex biological systems, where assays are required to be highly robust if they are to be of use. More cutting-edge assays have used dielectric-core metal-coated nanoshells bioconjugated to antibodies [1, 25–27]. These assays produce excellent sensitivity combined with low levels of undesired biological interaction between the label and the analyte. However, with the nanoshells free in solution, SERS spectra can be difficult to reproduce unless the analyte is spun down using centrifugation or immobilized in some manner; these processes can be damaging to some biological samples.

Scientists in a broad variety of fields continue to exploit various forms of nanostructures inspired by Nature [28]. Naturally occurring nanostructures that have evolved for functions involving visual appearance have been the subject of a remarkable surge in research interest [29–33]. This has built upon a range of somewhat earlier studies [34, 35]. Numerous insects, birds and plants exhibit a wide array of complex periodic and quasi-periodic ultrastructure. Their nanostructures can contribute to many biological functions: highly unsaturated color appearances for short- or long-range conspecific communication [36, 37]; angle-independent color [38] and specular or diffuse broadband appearances [39] for specialized camouflage; linearly [36] or circularly polarized re-

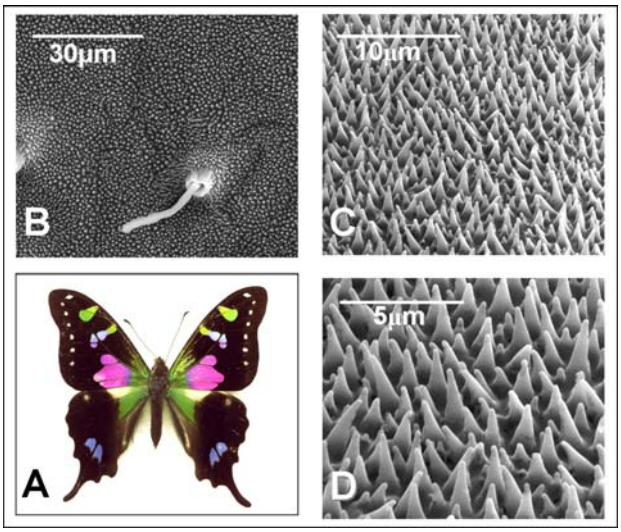

Figure 1 (online colour at: www.biophotonics-journal.org) *G. weiskei* butterfly wings and scanning electron microscope (SEM) micrographs of their detailed nanostructure at different magnifications.

flection [40] for high-level communication, represent a few of these. A recent investigation into the optical properties of cicada wings found that the "quasiperiodic" nanostructured anti-reflective coating on the chitinous wing surfaces provided an excellent SERS substrate, with enhancement factors of approximately 10^6 [41].

Avidin and biotin provide a model protein-binding system analogous to antibody/antigen binding, and are chosen for use in many immunoassays because they are well characterized, have high specificity and an almost unparalleled binding strength [42–44]. In this study, we demonstrate that conical cuticular nanostructures found on the metallicized surface of the *Graphium weiskei* butterfly (Figure 1) display ideal properties for avidin/biotin assaying using SERS. They exhibit excellent biocompatibility due to the possibility for optimal hydration conditions. We show that synthetic replicas of these nanostructures can be produced by a simple application of reactive ion etching, a process that is adaptable, tunable and suitable for economical large-scale fabrication. These biomimetically conceived substrates exhibit equally sensitive surface enhancement and biocompatibility to the wing substrates.

2. Experimental

The SERS enhancement factors were ascertained using self-assembled thiophenol monolayers as a well-defined model system. The biocompatibility of the butterfly wing substrates was demonstrated by obtaining SERS spectra of avidin glycoproteins bound to the functionalized metal surface whilst under aqueous buffer. To show the potential application of these substrates for detection of low concentrations of analyte, a reproducible wet binding assay was undertaken with varying concentrations of biotin in solution. Biotin and avidin were chosen as a model system as they have similar environmental requirements to other assay proteins, are well characterized and are widely used in biomedical research because of their very low dissociation constant ($K_D \sim 10^{-5}$ M). Normal hydrated avidin and avidin/biotin Raman spectra were obtained for comparison with SERS spectra.

2.1 Preparation of natural nanostructures

Male *G. weiskei* butterflies were purchased from World Wide Butterflies Ltd (wwb.co.uk). The specific wing areas of *G. weiskei* butterflies exhibiting conical nanostructures (see Figures 1 and 2) were dissected and cut into 2 × 2 mm sections that were attached to standard glass microscope slides using Norland Optical Adhesive (Cranbury, USA). All glassware was cleaned with aqua regia (concentrated hydrochloric acid mixed with concentrated nitric acid in a 3:1 ratio), rinsed exhaustively with nanopure water (PURITE, Oxford, UK) and subsequently rinsed with absolute ethanol and dried prior to use.

The adhesive was cured using a UV spot curing system (Novacure, USA) and kept in an incubator at 50 °C overnight to facilitate covalent bonding between the glass and the adhesive. A continuous film of either gold or silver (99.999% purity, GMBH) was then thermally evaporated over the wing surface at 10^{-6} mBar using a custom-built resistance-heated vacuum thermal evaporator, at deposition rates of between 1 nm s^{-1} and 0.5 nm s^{-1}. The thickness of the metal films and the deposition rates were monitored using a quartz microbalance crystal, and were later verified using atomic force microscopy (Ntegra

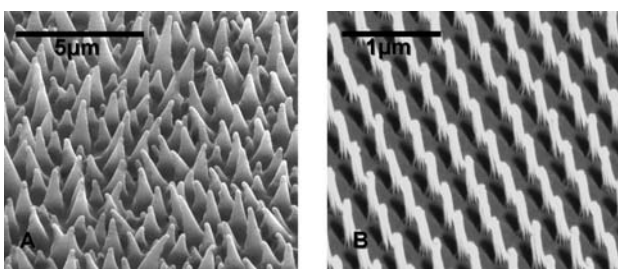

Figure 2 SEM micrographs of the *G. weiskei* nano-cone arrays (A) and the biomimetic substrate (B), with nano-cone heights of 524 nm peak-to-peak distances of 390 nm.

NT-MDT, Russia). Various metal thicknesses were investigated, ranging from 10–100 nm.

2.2 Fabrication of biomimetic nanostructures

Biomimetic nanostructured surfaces were prepared using the procedure previously reported by Weekes et al. [45]. Briefly, glass substrates were spin coating with a 1.5 μm thick layer of PMMA that was then annealed at 180 °C. An hexagonally ordered monolayer of 390 nm diameter polystyrene microspheres was then applied and used as a mask for reactive-ion etching (RIE). Reactive ion etching was applied for 8 min in an oxygen plasma produced by a 15 W RF source at a base pressure of oxygen of 50 mTorr. The process left a regular array of nanoscale pillars as shown in Figure 2, with the total height of the pillars equal to the sum of thickness of the PMMA layer and the height of the remaining spheres after etching (~0.5 μm). The width of the pillars was measured as 0.3 μm. Substrates were then metallicized using the procedure described in the previous section.

2.3 Imaging and spectroscopy

The butterfly wing regions were investigated by scanning electron microscopy (SEM) using a Hitachi S-3200N SEM. Prior to SEM, the samples were sputtered with 5 nm of chromium (for 3 min at 1 kV and 150 mTorr) in a Cressington sputter coater (208 HR). Raman spectra were acquired using a Renishaw RM1000 Raman microscope (RENISHAW, Wooton-Under-Edge, UK) equipped with a 1200-line/mm grating providing a spectral resolution of 1 cm^{-1}, a diode laser providing excitation at 785 nm with up to 300 mW power, and a 40 × microscope objective lens was used to focus light onto the substrate. The system was calibrated using the Raman band of a silicon wafer at 520 cm^{-1}. Spectral data was acquired using Renishaw v.1.2 WiRE software.

2.4 Thiophenol monolayers

The enhancement factors of the various substrates were quantified and compared using thiophenol. Thiophenol forms a highly repeatable and well-defined self-assembled monolayer with a well-characterized Raman and SERS spectra [46]. Monolayers were prepared using a modified version of the procedure described by Briand et al. [47]. Immediately after silver/gold deposition, the samples were immersed in absolute ethanol for 1 min, followed by immersion in an ethanolic solution of 10 mM thiophenol for 10 min. After formation of a thiophenol monolayer, the samples were rinsed in ethanol and allowed to dry under nitrogen before Raman analysis using a laser power of 3 mW. Enhancement factors were calculated using the ratio of SERS counts per molecule to that of the spontaneous Raman counts acquired from bulk thiophenol [41]. Raman spectra of the bare metal substrates were taken to determine the affect chitin/PMMA could have on the subsequent experiments.

2.5 Normal Raman spectra

Normal Raman spectra were obtained using solutions of avidin and avidin bound to biotin deposited onto quartz cavity slides. Spectra of these solutions were taken using 150 mW laser power.

2.6 Bioconjugation for model "immunoassay" system

A model immunoassay was performed by conjugating avidin onto the metallicized wing surfaces and using the SERS spectra to detect biotin binding as a function of biotin concentration. The metal-coated substrates were modified with self-assembled monolayers of a molecular linker (3-mercaptopropanoic acid – MPA); the substrates were immersed in an ethanolic solution of 0.02 M MPA for 2 h.

The MPA layer was activated using a solution of 2 mM ethyl dimethylaminopropyl carbodiimide (EDC) and 5 mM n-hydroxy succinimide (NHS) in 2-(*N*-morpholino) ethanesulfonic acid (MES) buffer solution (20 mM MES, 0.1 M NaCl, pH 5). The carboxylate groups of the MPA react with NHS in the presence of EDC to form NHS-esters that can then react with amine groups of proteins. After 15 min of activation, the metallicized samples were rinsed in phosphate buffered saline (PBS) at pH 7.50 μL aliquots of avidin solution (Sigma Aldrich) at 10 mg/mL in PBS at pH 7 were deposited onto each silvered wing section, and left to incubate for 30 min at 4 °C.

After incubation, the samples were rinsed in PBS pH 7 and immersed in a quenching solution of 1 M ethanolamine in PBS for 30 min at 4 °C to deactivate any unreacted NHS-esters. Following immersion in the quenching solution, the silvered samples were rinsed in PBS pH 7. Aliquots of biotin solutions over a range of concentrations were then added and allowed to bind for 20 min at 4 °C. The samples were

then rinsed in Millipore water (PURITE, Oxford, UK) and the active area kept hydrated under a droplet of PBS to prevent the proteins from denaturing.

The optimum laser power was determined by a laser power study: powers up to 100 mW caused no photodamage to the sample, so this was set as the maximum allowed laser power.

3. Results and discussion

3.1 Determining the enhancement factors

From spectra of the bare metal substrates it was determined that the chitin/PMMA contribution was negligible. This is because the surface-enhancement field decays evanescently with distance; the metal deposited upon the substrates was sufficiently thick that the chitin/PMMA SERS signal was overwhelmed by that from the metals upper surface.

To determine enhancement factors, the number of Raman counts per molecule in the SERS spectrum of the substrates was estimated by assuming that the thiophenol monolayer was at maximum density. The maximum coverage of alkanethiols on thermally evaporated gold substrates has been shown to be 21%; 2.5×10^{14} molecules/cm^2 $\pm$ 0.1×10^{14} molecules [48]. Assuming 100% metal coverage, this provides a conservative estimate for the enhancement factor, since the maximum density of monolayers of alkanethiols typically take 1–2 h to form. The area of the substrate illuminated by the objective was calculated from the Airy disc diameter; hence the number of thiophenol molecules in the focal area was estimated as $6.0 \times 10^6 \pm 1.3 \times 10^4$.

For the Raman spectrum of neat thiophenol (Figure 3), the number of Raman counts per molecule was estimated in a similar manner; the confocal sample volume of the microscope objective, calculated from the diameter of the Airy disc over the axial response arising from a pinhole of size 10 micrometers, was found to be $1.13 \times 10^{-2} \pm 7.94 \times 10^{-5}$ picolitres. For neat thiophenol, this corresponds to $6.6 \times 10^{10} \pm 4.8 \times 10^8$ molecules.

For the SERS spectra of the thiophenol monolayers (Figure 3), peak assignments of the most prominent Raman bands were made based on Refs. [49, 50] as follows; 1574 cm^{-1} (C–C stretching); 1072 cm^{-1} (inplane C–C–C stretch and C–S stretching); 1022 cm^{-1} (out-of-plane C–H stretching); 999 cm^{-1} (out-of-plane C–C–C stretch); 630 cm^{-1} (out-of-plane C–C–C and C–S stretching). Enhancement factors were calculated using the peak heights at 999 cm^{-1} of the monolayers compared with the nonenhanced 1001 cm^{-1} peak of thiophenol in solution.

When corrected for acquisition times and any variations in laser powers used, the maximum enhancement factors for the metallicized *G. weiskei* wing surfaces were found to be $1.9 \times 10^6 \pm 5.8 \times 10^4$ for gold, and $1.6 \times 10^7 \pm 1.8 \times 10^5$ for silver. For the biomimetic substrates, the maximum enhancement factors were $1.1 \times 10^6 \pm 5.1 \times 10^4$ for gold and $1.4 \times 10^7 \pm 1.7 \times 10^5$ for silver. We found that the optimum enhancement factors for silver and gold occurred at different thicknesses (70 nm and 90 nm, respectively). This is because their different dielectric functions led to different surface plasmon properties, a fact that has been exploited to tune core-shell nanoparticles to preferentially absorb light at specific wavelengths [1, 26, 27].

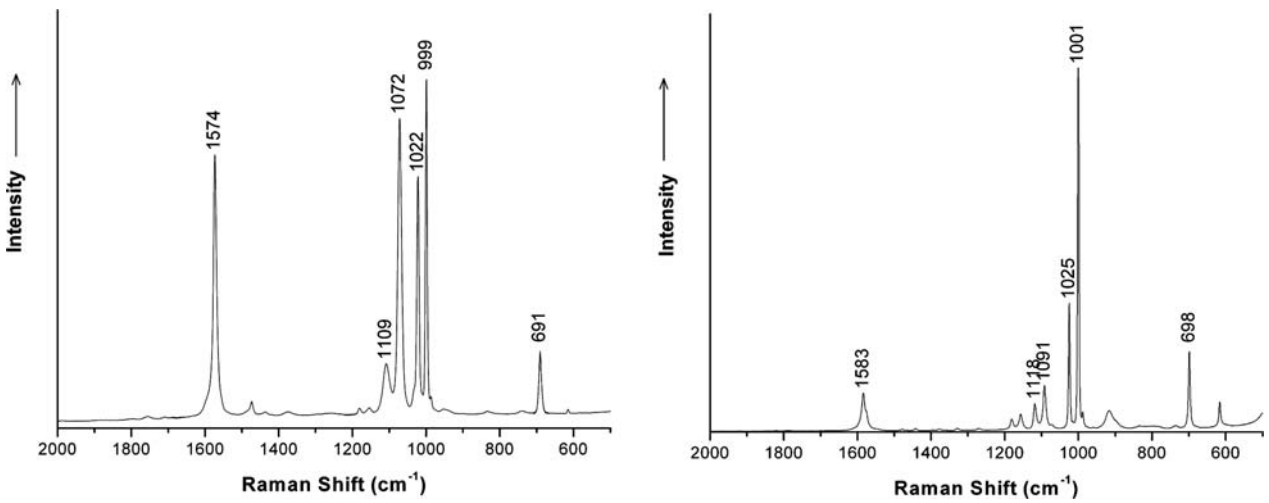

Figure 3 SERS spectra of a thiophenol monolayer on a butterfly wing coated with 70 nm silver (left) and an un-enhanced Raman spectrum of neat thiophenol in solution (right).

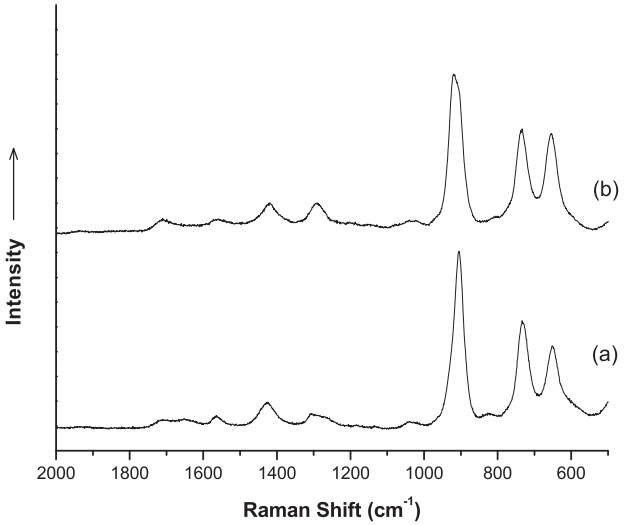

Figure 4 SERS spectra of MPA a) prior to activation with EDC/NHS, b) after activation.

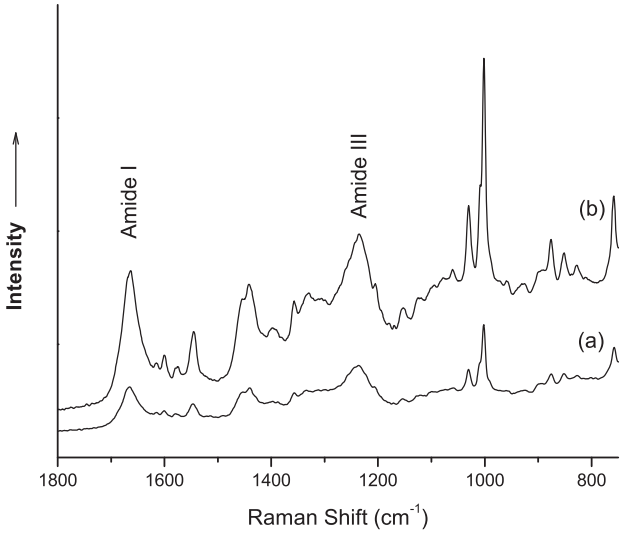

Figure 5 Normal Raman spectra for avidin (a) and avidin-biotin (b).

3.2 Bioconjugation

The MPA molecule binds to metal surfaces via a covalent bond from the sulfur group. If the concentration of MPA molecules on a metal surface is high, the molecules tend to orient themselves in a *trans*-configuration, whereas if the concentration is low, the MPA molecules will have a higher instance of *gauche*-configuration. These conformational changes result in distinctive changes in their SERS spectra, which can be seen in Figure 4. In the *gauche*-configuration, the protein-binding site of the MPA molecule is less accessible than those in the *trans*-configuration; the optimal MPA deposition time was determined by performing depositions for a range of times and comparing the ratios of the *gauche* and *trans* peaks (at 654 cm^{-1} and 735 cm^{-1}, respectively) [51–53]. Upon activation of the MPA monolayer, the carboxyl band at 900 cm^{-1} shifts to 928 cm^{-1}, indicating that the carboxyl group has become dissociated.

3.3 Normal spectra

The most prominent peaks in the hydrated avidin Raman spectrum (see Figure 5) were tentatively assigned to phenylalanine (1001 cm^{-1}, 1030 cm^{-1}), tryptophan (759 cm^{-1}, 875 cm^{-1}, 930 cm^{-1}, 960 cm^{-1}, 1001 cm^{-1}, 1357 cm^{-1}, 1546 cm^{-1} and 1580 cm^{-1}), tyrosine (827 cm^{-1}, 852 cm^{-1}), C–C stretching (930 cm^{-1}), COO symmetric stretching (1400 cm^{-1}). The amide I and amide III regions were located at 1665 cm^{-1} and 1237 cm^{-1}, respectively. Each avidin peak lay within 6 cm^{-1} of the same peak assignments for the lyophilated avidin spectrum reported by Fagnano at al. [44]. A 6 cm^{-1} discrepancy is reasonable given the conformational changes that can occur between hydrated and lyophilised proteins, combined with the 2–3 cm^{-1} limit of resolution of the system.

It was found that upon binding to biotin, the 960 cm^{-1} tryptophan peak increased relative to the 1001 cm^{-1} phenylalanine peak (see Figure 5), as reported by Fagnano et al. [44]. Since the avidin binding site contains the amino acids phenylalanine, alanine, asparagine and tryptophan [54], the 960 cm^{-1} tryptophan peak and the 1001 cm^{-1} phenylalanine peak were chosen as binding indicator peaks for investigation in the SERS assay. The amide I and amide III bands did not change significantly upon addition of biotin.

3.4 SERS assay

Once avidin molecules were bound to an MPA monolayer, SERS spectra were acquired over the region of interest (see Figure 6). These spectra showed weak contributions from MPA at 654 cm^{-1}, 735 cm^{-1} and 925 cm^{-1}. The following peaks corresponded with those identified in the normal spectrum of avidin: 833 cm^{-1} and 848 cm^{-1} (tyrosine), 925 cm^{-1} (C–C stretching/MPA carboxyl group), 1001 cm^{-1} and 1028 cm^{-1} (phenylalanine), 1237 cm^{-1} (amide III) and 1394 cm^{-1} (COO symmetric stretching). Several peaks were identified that did not correspond with the normal spectrum of avidin, most likely due to the different selection rules for SERS. These were tentatively assigned using the SERS spectra of individual amino acids reported by Stewart and Freder-

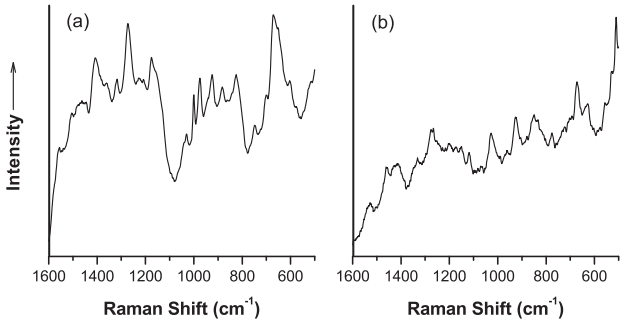

Figure 6 SERS spectra of avidin bound to gold-coated wing (b) and the avidin-biotin complex bound to gold-coated wing (a).

icks [55]: 1494 cm^{-1} (tryptophan), 1332 cm^{-1} and 1289 cm^{-1} (glutamine).

Upon addition of biotin, the two peaks in the avidin-biotin complex spectra that were indicative of the complex formation were found to be 975 cm^{-1} and 1000 cm^{-1}. Given that the Raman peaks of individual amino acids may be expected to shift with surface enhancement, we assigned the 975 cm^{-1} avidin SERS peak to tryptophan and the 1000 cm^{-1} avidin SERS peak to phenylalanine.

It was found that the 1000 cm^{-1} peak decreased in strength relative to the 975 cm^{-1} peak with increasing biotin concentration as illustrated in Figure 7. This attribute was exploited to perform a biotin assay (see Figure 8). The log plot of the assay gave a linear response over a range of 0.5–1000 nM (equivalent to 0.12 ng/mL – 0.24 μg/mL) solutions

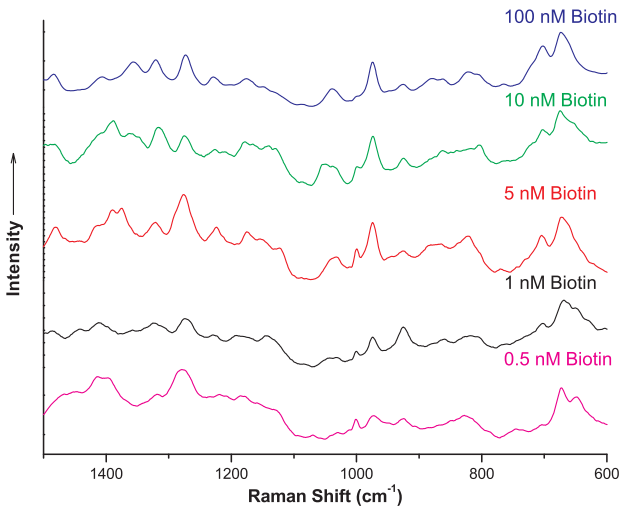

Figure 7 (online colour at: www.biophotonics-journal.org) A comparison of the different SERS spectra obtained during the biotin assay (the concentration of biotin added is given for each spectrum). The peak at 975 cm^{-1} was found to increase relative to the peak at 1000 cm^{-1} with increasing biotin concentration.

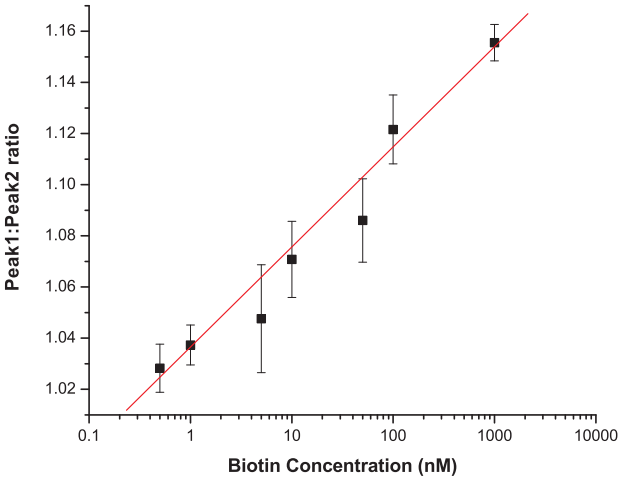

Figure 8 (online colour at: www.biophotonics-journal.org) Ratios of the heights of the peaks at 975 cm^{-1} (peak 1) and 1000 cm^{-1} (peak 2) in the SERS spectra of the avidin-biotin complex for gold-coated butterfly wings for a range of concentrations of biotin in buffer solution.

of biotin suspended in buffer solution. The limit of detection of this assay was 0.2 nM (49 pg/mL).

4. Discussion

We have demonstrated that butterfly wing nanostructures can provide an excellent SERS substrate for use with protein assaying without the need for desiccating the sample – a major advantage over other nanostructures surfaces used as SERS substrates. The entire avidin/biotin assay took no more than 4 h from surface conjugation to SERS scanning, which is comparable to some of the more rapid ELISA assays commercially available. The volume of analyte used was very small (only 30 μL), which would be an advantage for applications in areas such as forensics where it is often impractical or impossible to perform assays on large volumes of analyte.

One of the main advantages of our SERS assay was the large range of analyte concentrations that could be used (0.12 ng/mL–0.24 μg/mL) without the need for dilution of the analyte, as illustrated in Figure 8. Until now, SERS assays have been effective over typical analyte concentration ranges spanning only one to two orders or magnitude [1, 2, 21, 22, 27], while ELISA assays have been made with effective concentration ranges of pg/ml to ng/mL [4]. Our assay technique has bridged the gap between SERS and ELISA assays, potentially paving the way for commercially viable SERS substrates for undertaking assays of wet biological samples. Since SERS

provides detailed structural and chemical information about assay analytes, with effective concentration detection ranges as large as those used in ELISA, SERS could become a much more effective immunoassay choice.

In order to demonstrate the potential for mimicking the conical nanostructures of the butterfly wings for commercial applications, a simple reactive-ion-etching technique was employed. Since the wing nanostructure exhibited quasiperiodicity and a range of cone sizes and orientations, an exact duplicate of this structure was beyond the scope of this technique. Nonetheless, the biomimetic substrates showed excellent SERS enhancement factors (1.1×10^6 with a 90 nm coating of gold and 1.4×10^7 for a 70 nm coating of silver). Preliminary biocompatibility experiments showed that these substrates exhibit the remarkable property of enabling SERS signals to be obtained when the scanning area is submerged under a droplet of buffer solution.

Future experiments will focus on combining these biomimetic substrate production techniques with nanotransfer printing methods in order to speed up production times and reduce costs, for use with biological applications.

5. Conclusion

We have shown that naturally occurring nanostructures and their biomimetic analogues produced excellent SERS substrates when coated with gold or silver. The butterfly wing substrates used for a wet biotin assay were found to be sensitive over a concentration range comparable with ELISA. The excellent biocompatibility of the wings and biomimetic substrates is unparalleled by other lithographically produced substrates, and this could pave the way for widespread application of ultrasensitive SERS-based bioassays.

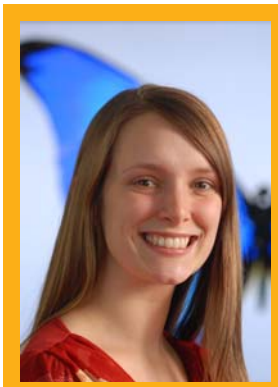

Natalie L. Garrett obtained first class honours for her MPhys in Physics with Medical Physics at the University of Exeter in 2006 and is now working on her PhD in the University of Exeters Biomedical Physics research group. Her research involves biomedical applications of various spectroscopic techniques including Raman, SERS and CARS.

Peter Vukusic graduated from the University of Exeter in 1993 with a PhD in Optical Physics. He began to investigate structural color in natural systems in 1998 and in 2003 was appointed permanent lecturer at the University of Exeters School of Physics. His research group undertakes work that comprises discovery, characterization and technological application of the unique optics and photonics systems that have evolved naturally in animals and plants. This work is frequently featured on scientific programs of the BBC and National Geographic.

Evgeny Sirotkin graduated from Saratov State University, Russia in 2006 with a Masters Degree in Solid State Physics and specialization "Microelectronics and semiconductor devices". He is currently a PhD student in nanomagnetics at the School of Physics at the University of Exeter. The field of his present research at Exeter University is fabrication and micromagnetic characterizations of large-area highly ordered arrays of ferromagnetic nanoelements. His main scientific interests are: nanomagnetism, patterned magnetic media, fabrication of nanostructures and self-assembling.

Feodor Y. Ogrin graduated form Moscow Institute of Physics and Technology (State University) in 1993 with a Masters Degree and later obtained his PhD in Physics from Keele University in 1996. Following a postdoctoral appointment at the University of St. Andrews, he became a Lecturer at School of Physics of the University of Exeter in 2001. Current research interests include studies of local magnetic structure in patterned magnetic media using soft X-ray/neutron scattering technique and micromechanics for biomedical applications (ferromagnetic microswimmers, magnetic micromotors).

C. Peter Winlove has been Professor of biophysics and Head of the Biomedical Physics Group at Exeter since 2000. He had previously been Reader in Connective Tissue Biophysics at Imperial College, London, where he obtained his first degree in theoretical physics. He obtained a D.Phil in quantum gravity before moving into biophysics. His current research interests include biophotonics, particularly it applications in physiology and medicine, and the physical properties of extracellular matrix macromolecules and membranes.

Julian Moger studied physics at the University of Exeter and obtained his PhD in 2003 with a thesis on Doppler Optical Coherence Tomography (DOCT). In 2005 he became a lecturer in the Biophysics Group at Exeter. His research concerns the development of novel biophotonic techniques with a wide range of applications. He has developed and is currently managing a multiphoton imaging and spectroscopy laboratory, a field in which his research is currently focused.

References

[1] S. P. Xu, X. H. Ji, W. Q. Xu, B. Zhao, X. M. Dou, Y. B. Bai, and Y. Ozaki, J. Biomed. Opt. **10**, 031112-1–031112-12 (2005).
[2] X. Dou, T. Takama, Y. Yamaguchi, H. Yamamoto, and Y. Ozaki, Anal. Chem. **69**, 1492 (1997).
[3] A. Ronald and W. H. Stimson, Parasitology **117**, 13 (1998).
[4] J. P. Gosling, Clin. Chem. **36**, 1408 (1990).
[5] J. Moger, P. Gribbon, A. Sewing, and C. P. Winlove, J. Biomolec. Screen. **11**, 765 (2006).
[6] M. Fleischman, P. J. Hendra, and A. J. McQuilla, Chem. Phys. Lett. **26**, 163 (1974).
[7] J. Moger, P. Gribbon, A. Sewing, and C. P. Winlove, Biochim. Biophys. Acta-General Subjects **1770**, 912 (2007).
[8] S. M. Nie, in: Abstracts of Papers of the American Chemical Society (American Chemical Society, Washington DC, 2001) U244-U244.
[9] S. J. Lee, A. R. Morrill, and M. Moskovits, J. Am. Chem. Soc. **128**, 2200–2201 (2006).
[10] P. C. Lee and D. Meisel, J. Phys. Chem. **86**, 3391–3395 (1982).
[11] M. G. Albrecht and J. A. Creighton, J. Am. Chem. Soc. **99**, 5215 (1977).
[12] D. L. Jeanmaire and R. P. van Duyne, J. Electroanal. Chem. **84**, 1 (1977).
[13] D. G. Duff, A. Baiker, and P. P. Edwards, Langmuir **9**, 2301 (1993).
[14] D. G. Duff, A. Baiker, I. Gameson, and P. P. Edwards, Langmuir **9**, 2310 (1993).
[15] D. J. White, A. P. Mazzolini, and P. R. Stoddart, J. Raman Spectrosc. **38**, 377 (2007).
[16] T. R. Jensen, M. D. Malinsky, C. L. Haynes, and R. P. Van Duyne, J. Phys. Chem. B **104**, 10549–10556 (2000).
[17] S. E. Hunyadi and C. J. Murphy, J. Mater. Chem. **16**, 3929 (2006).
[18] M. E. Abdelsalam, P. N. Bartlett, J. J. Baumberg, S. Cintra, T. A. Kelf, and A. E. Russell, Electrochem. Commun. **7**, 740 (2005).
[19] G. A. Baker and D. S. Moore, Anal. Bioanalyt. Chem. **382**, 1751 (2005).
[20] M. L. Zhang, C. Q. Yi, X. Fan, K. Q. Peng, N. B. Wong, M. S. Yang, R. Q. Zhang, and S. T. Lee, Appl. Phys. Lett. **92**, (2008).
[21] X. Dou, Y. Yamaguchi, H. Yamamoto, S. Doi, and Y. Ozaki, J. Raman Spectrosc. **29**, 739 (1998).
[22] S. P. Xu, L. Y. Wang, W. Q. Xu, B. Zhao, H. Yuan, L. Ma, Y. B. Bai, and Y. G. Fan, Chem. J. Chin. Univ. – Chinese **24**, 900 (2003).
[23] Y. Levy and J. N. Onuchic, Ann. Rev. Biophys. Biomolec. Struct. **35**, 389 (2006).
[24] C. Ortiz, D. Zhang, Y. Xie, A. E. Ribbe, and D. Ben-Amotz, Anal. Biochem. **353**, 157 (2006).
[25] T. E. Rohr, T. Cotton, N. Fan, and P. J. Tarcha, Anal. Biochem. **182**, 388 (1989).
[26] L. R. Hirsch, J. B. Jackson, A. Lee, N. J. Halas, and J. West, Anal. Chem. **75**, 2377 (2003).
[27] X. Ji, S. Xu, L. Wang, M. Liu, K. Pan, H. Yuan, L. Ma, W. Xu, J. Li, Y. Bai, and T. Li, Colloids Surfaces A: Physicochem. Eng. Aspects **257–258**, 171 (2005).
[28] R. M. Alexander, Nature **438**, 166 (2005).
[29] P. Vukusic and J. R. Sambles, Nature **424**, 852 (2003).
[30] M. Srinivasarao, Chem. Rev. **99**, 1935 (1999).
[31] R. A. Potyrailo, H. Ghiradella, A. Vertiatchikh, K. Dovidenko, J. R. Cournoyer, and E. Olson, Nature Photon. **1**, 123 (2007).
[32] A. R. Parker in: Functional Morphology of the Invertebrate Skeleton, edited by E. Savazzi (John Wiley & Sons Ltd., New York, 1999).
[33] S. Kinoshita, S. Yoshioka (eds.), Structural Colors in Biological Systems: Principles and Applications (Osaka University Press, Osaka, 2005).
[34] M. F. Land, Prog. Biophys. Molec. Biol. **24**, 75 (1972).
[35] H. Ghiradella, D. Aneshansley, T. Eisner, R. E. Silberglied, and H. E. Hinton, Science **179**, 415 (1973).
[36] P. Vukusic, R. J. Wootton, and J. R. Sambles, in: Proc. Roy. Soc. London Series B-Biol. Sci. (Royal Society London, London, 2004), pp. 595–601.

[37] S. Yoshioka and S. Kinoshita, Opt. Exp. **15**, 2691 (2007).
[38] P. Vukusic, R. Sambles, C. Lawrence, and G. Wakely, Appl. Opt. **40**, 1116 (2001).
[39] P. Vukusic, B. Hallam, and J. Noyes, Science **315**, 348 (2007).
[40] S. A. Jewell, P. Vukusic, and N. W. Roberts, New J. Phys. **9** (2007).
[41] P. R. Stoddart, P. J. Cadusch, T. M. Boyce, R. M. Erasmus, and J. D. Comins, Nanotechnology **17**, 680 (2006).
[42] R. J. Pei, Z. L. Cheng, E. K. Wang, and X. R. Yang, Biosens. Bioelectron. **16**, 355 (2001).
[43] O. Livnah, E. A. Bayer, M. Wilchek, and J. L. Sussman, in: Proc. Nat. Acad. Sci. USA **90**, 5076 (1993).
[44] C. Fagnano, G. Fini, and A. Torreggiani, J. Raman Spectrosc. **26**, 991 (1995).
[45] S. M. Weekes, F. Y. Ogrin, W. A. Murray, and P. S. Keatley, Langmuir **23**, 1057 (2007).
[46] J. Pate, A. Leiden, B. J. Bozlee, and R. L. Garrell, J. Raman Spectrosc. **22**, 477 (1991).
[47] E. Briand, M. Salmain, J. M. Henry, H. Perrot, C. Compere, and C. M. Pradier, Biosens. Bioelectron. **22**, 440 (2006).
[48] C. O'Dwyer, G. Gay, B. Viaria de Lesegno, J. Weiner, M. Mützel, D. Haubrich, D. Meschede, K. Ludolph, G. Georgiev, and E. Oesterschulze, J. Phys.: Conf. Ser. **19**, 109 (2005).
[49] M. A. Bryant and J. E. Pemberton, J. Am. Chem. Soc. **113**, 3629 (1991).
[50] M. A. Bryant and J. E. Pemberton, J. Am. Chem. Soc. **113**, 8284 (1991).
[51] A. Michota, A. Kudelski, and J. Bukowska, Surf. Sci. **502**, 214 (2002).
[52] A. Kudelski, Surf. Sci. **502**, 219 (2002).
[53] A. Kudelski and W. Hill, Langmuir **15**, 3162 (1999).
[54] T. S. Huang and R. J. Delange, J. Biol. Chem. **246**, 686 (1971).
[55] S. Stewart and P. M. Fredericks, Spectrochim. Acta Part A – Molec. Biomolec. Spectrosc. **55**, 1641 (1999).

